ENERGY DISSIPATION ON FLAT-SLOPED STEPPED SPILLWAYS: PART 1. UPSTREAM OF THE INCEPTION POINT

S. L. Hunt, K. C. Kadavy

ABSTRACT. *In recent years, hazard classifications for many existing embankment dams have changed because hydrologic conditions have been altered. Consequently, many of these dams no longer provide adequate spillway capacity according to state and federal dam safety regulations. Stepped spillways are a popular choice for providing increased spillway capacities to existing embankment dams. Stepped spillways in these applications are typically placed over the existing embankment or auxiliary spillway; thereby, the chute slope is the same as the downstream embankment face or auxiliary spillway slope. Design guidelines and literature in general for these stepped spillways are very limited, so further research on these stepped spillways is warranted. A two-dimensional, physical model was constructed to evaluate the inception point, velocities, and energy dissipation in a 4(H):1(V) spillway chute having 38 mm (1.5 in.) high steps. Model unit discharges ranging from 0.11 $m^3 s^{-1} m^{-1}$ (1.2 cfs ft^{-1}) to 0.82 $m^3 s^{-1} m^{-1}$ (8.8 cfs ft^{-1}) were tested. Water surfaces, bed surfaces, and velocities were collected during the tests. An inception point relationship provided by H. Chanson may be used to determine the inception point for slopes as flat as 4(H):1(V) when F_* ranges between 10 and 100. The velocity profiles transition from uniform at the crest to approaching a one-sixth power law distribution at the inception point for all tested flows. Energy losses increase in a linear fashion from near zero at the crest to approximately 30% near the inception point for all tested flows. This research will assist engineers with the design of stepped spillways applied on relatively flat embankment dams.*

Keywords. *Air entrainment, Dam rehabilitation, Energy dissipation, Flood control, Inception point, Physical modeling, Roller compacted concrete (RCC), Stepped spillways, Stilling basin.*

Roller compacted concrete (RCC) stepped spillways have grown in popularity over the years because of their feasibility and because of their ease of construction when compared to other design solutions. Additionally, these structures provide substantial energy dissipation, thereby allowing for shorter stilling basins. Stepped spillways are commonly being used to bring existing embankments into compliance with state and federal dam safety regulations. For instance, several existing flood control dams are faced with hazard classification changes due to urbanization. As a result, the existing spillway capacity is not compliant with the new hazard classification change. Roller compacted concrete stepped spillways provide a means to increase spillway capacity without necessarily causing other modifications to the dam dimensions (i.e., top of dam elevation). In these cases, the stepped spillways are typically placed over the existing earthen embankment or auxiliary spillway; thus, the slope of the spillway chute is most often defined by the downstream slope of the embankment or by the slope of the existing auxiliary spillway. Typical slopes for these embankments are 2(H):1(V) or flatter. Stepped spillway research for these flatter applications has been quite limited, and design guidelines are scarce.

The USDA Agricultural Research Service (ARS) Hydraulic Engineering Research Unit (HERU) has focused research in the area of stepped spillways applied to existing embankment dams. Questions regarding air entrainment and energy dissipation on flat-sloped stepped spillways and spillway convergence have been among the most prominent design inquiries due to the effect that these elements have on the design and performance of the overall structure. It is these areas of interest that researchers at HERU are investigating in order to provide more definitive design guidelines to engineers faced with these design challenges. The USDA-ARS HERU is currently working on a generalized model study to evaluate the effects that a 4(H):1(V) sloped stepped spillway chute has on the inception point, the energy dissipation, and velocities for a given range of flows. The objective of this work is to discuss velocity and energy dissipation findings upstream of the air entrainment inception point for a 4(H):1(V) stepped spillway with 38 mm (1.5 in.) steps.

Submitted for review in April 2009 as manuscript number SW 7984; approved for publication by the Soil & Water Division of ASABE in December 2009. Presented at the 2008 ASABE Annual Meeting as Paper No. 084151.

The authors are **Sherry L. Hunt, ASABE Member Engineer,** Research Hydraulic Engineer, and **Kem C. Kadavy, ASABE Member Engineer,** Agricultural Engineer, USDA-ARS Hydraulic Engineering Research Unit, Stillwater, Oklahoma. **Corresponding author:** Sherry L. Hunt, USDA-ARS Hydraulic Engineering Research Unit, 1301 N. Western St., Stillwater, OK 74075; phone: 405-624-4135, ext. 222; fax: 405-624-4136; e-mail: Sherry.Hunt@ars.usda.gov.

BACKGROUND

Stepped chute technology is not new. In fact, Chanson (2002) dates the technology back to 1300 B.C. in ancient Greece. Yet design guidelines are still limited, even more so for the flatter sloped (2(H):1(V) or flatter) stepped spillways associated with small embankment dams. Generalized investigations of the hydraulic performance of stepped spillways have been conducted by several researchers. Many

of these research studies were performed on steeper (2(H):1(V) or steeper) stepped spillways, but a few researchers, including Peyras et al. (1992), Rice and Kadavy (1996), Yasuda and Ohtsu (1999), Chanson and Toombes (2002), Boes and Hager (2003a, 2003b), Gonzalez (2005), Takahashi et al. (2006), Hunt and Kadavy (2007, 2008), and Felder and Chanson (2008), have examined flat-sloped (2(H):1(V) or flatter) stepped spillways.

Important elements in stepped spillway and stilling basin design are the location of the inception point in the spillway chute and the energy dissipation that occurs in the chute. The inception point, as defined by Chanson (1994a, 2002), is the location where the turbulent boundary layer reaches the free surface. Figure 1 illustrates the inception point in relation to the broad-crested weir in a stepped spillway. Factors such as the inception point and energy dissipation ultimately affect the spillway training wall design and the stilling basin dimensions. Chanson (1994a) made significant strides under skimming flow conditions by distinguishing differences between flow patterns on steep and flat stepped chutes. Chanson (1994b) also developed a relationship for predicting the inception point location from research conducted primarily on steep (2(H):1(V) or steeper) stepped chutes, and Hunt and Kadavy (2007, 2008) and Hunt et al. (2006) show promise that the inception point relationship developed by Chanson (1994b, 2002) will predict the inception point location on 3(H):1(V) and 4(H):1(V) stepped spillways. Christodoulou (1993) discovered that the most important parameters governing energy dissipation are the ratio of the critical depth to the step height and the number of steps. Christodoulou's (1993) research was conducted on a 0.7(H):1(V) stepped spillway. Boes (1999), Chanson (2002), and Chanson and Toombes (2002) have conducted extensive research on energy dissipation in stepped spillways; however, much of what was reported pertains to energy losses downstream of the inception point in regions of highly air-entrained flows. This article provides velocity and energy loss data upstream of the inception point for a range of flows in a generalized model study of a 4(H):1(V) stepped spillway. The benefits of this work are: (1) it provides design engineers with the knowledge of whether to take air entrainment into account for spillway training wall design, and (2) it provides a relationship upstream of the inception point for determining energy dissipation, a parameter used for stilling basin design. This research is important for the design of stepped spillways applied to small embankment dams because fully developed air-entrained flow is not always expected in these applications.

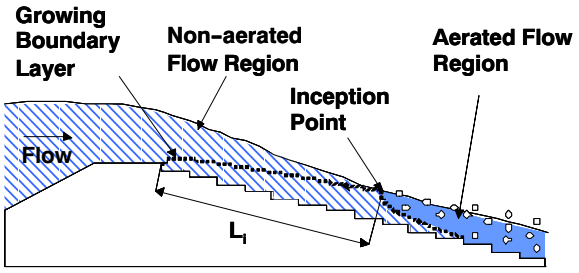

Figure 1. Schematic of the inception point in relation to the stepped spillway.

Experimental Setup

Viscous forces and surface tension in most open-channel applications are deemed negligible, but in highly air-entrained flows like those expected in stepped spillways, these forces are more dominating and cannot be simply ignored. If these forces are disregarded, then scale effects can occur, causing data misinterpretation. Boes (2000), Chanson (2002), Boes and Hager (2003a), and Takahashi et al. (2005) have well-documented scale effects that can occur in modeling stepped spillways. Scale effect is a term used to describe slight distortions that are introduced by ignoring secondary forces (i.e., viscous forces, surface tension) in these types of models. Scale effects in stepped spillway models are more commonly associated with scales smaller than 10:1. Chanson (2002), Boes and Hager (2003a), and Takahashi et al. (2006) have provided guidance for minimizing scale effects. Chanson (2002) recommends a model scale of 10:1 or larger, and Boes and Hager (2003a) proposes a minimum Reynolds number of 10^5 and a minimum Weber number of 100. Takahashi et al. (2006) recommends that Froude, Reynolds, and Morton similarity be satisfied for modeling highly air-entrained flow, but they recognize that this can only be achieved at full scale. A consensus among researchers has not been reached for the limits to minimize scale effects in physical models of stepped spillways, but some guidance is available.

A two-dimensional model of a stepped spillway was constructed for a generalized study to evaluate the inception point, velocities, and energy losses associated with flood flows. Figure 2 illustrates a schematic of the two-dimensional model. The stepped spillway was constructed with a broad-crested weir with the downstream edge of the weir corresponding to station 0.0 m and step 0, as shown in figure 2. The spillway slope is 4(H):1(V), and the step height is 38 mm (1.5 in.). The model was constructed across the full width of a 1.8 m (6 ft) flume. The flume walls are 2.4 m (8 ft), and the spillway model has a vertical drop of 1.5 m (5 ft). Figure 3 is a photo of the two-dimensional model as it was constructed in the test flume. A moveable carriage set atop rails on the flume walls allowed manual point gauge readings of the water and bed surfaces to be collected. This carriage was also used in velocity measurements along the crest section. A second set of rails was attached to the inside of the flume walls and set parallel to the chute slope. These rails were used to collect velocity profiles normal to the spillway chute along the centerline. Figure 4 illustrates the use of the carriage for recording flow measurements. The model unit discharges tested, along with the Reynolds and Weber numbers and the average velocity at the inception point, are summarized in table 1. The Reynolds and Weber numbers are well within the recommended guidelines set forth by Boes and Hager (2003a), and a scale of 10:1 or larger is recommended.

Velocities profiles and flow depths were collected along the centerline of the spillway using three separate measuring devices: (1) an acoustic Doppler velocimeter (ADV), (2) a pitot tube (PT) coupled with a differential pressure transducer, and (3) a two-tip fiber optical (FO) probe. Figure 5 shows the velocity instrumentation in use during the tests. Each device has a unique range of velocities that could be captured during testing. The ADV was limited by a maximum velocity of 4.6 m s^{-1} (15 ft s^{-1}), and it could not be

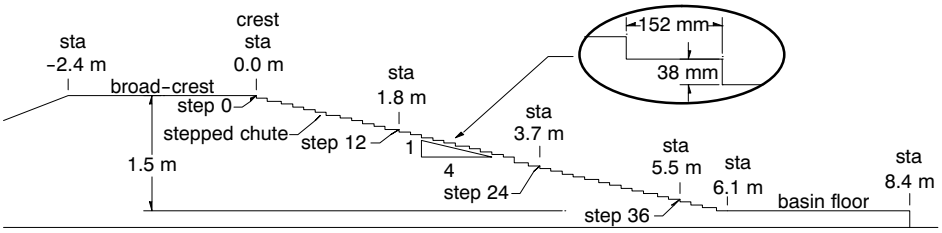

Figure 2. Schematic of stepped spillway model.

Figure 3. Two-dimensional stepped spillway model.

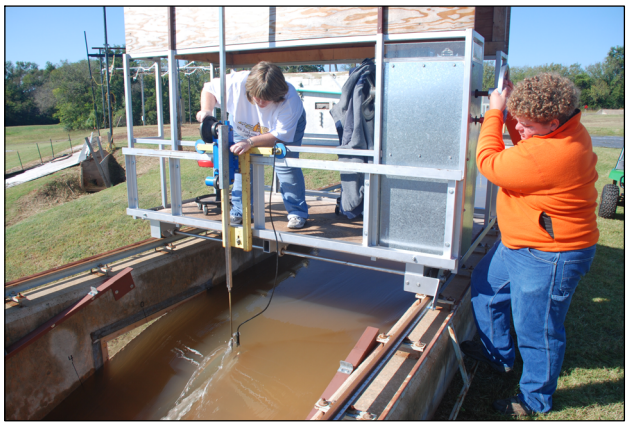

Figure 4. Data collection using the mobile carriage along the top of the test flume walls.

Table 1. Summary of unit discharge (q), Reynolds number (R), average velocity (V) at inception point, and Weber numbers (W).

q ($m^3\ s^{-1}\ m^{-1}$)	R	V ($m\ s^{-1}$)	W
0.11	9.59E+04	2.42	112
0.20	1.81E+05	3.08	142
0.28	2.50E+05	3.54	163
0.42	3.74E+05	4.02	186
0.62	5.49E+05	4.71	218
0.82	7.33E+05	5.06	234

used in situations of highly turbulent flow. The PT coupled with the pressure transducer handles larger velocities than the ADV and provides verification for some of the velocity results collected by the ADV. Although the PT is not usually recommended to measure velocities in highly air-entrained flows, Matos et al. (2002) found that it can be used in this environment when the air concentration in the flow is less than 70%. To achieve more accurate velocity measurement, the PT was back-flushed before each measurement. The two-tip FO probe measures velocities and void fractions in air-entrained flows, and it was used to collect the data downstream of the inception point. The air-entrained data are provided in Part 2 (Hunt and Kadavy, 2010). Velocity profiles were taken normal to the spillway crest surface along the centerline at stations -2.4, -1.8, -1.2, -0.61, 0.0 m (-8, -6, -4, -2, and 0 ft) with the ADV. Figure 2 illustrates the stations as they relate to the stepped spillway model. Additionally, cross-sectional velocity profiles were collected with the ADV at the broad-crested weir in order to develop a calibration curve to determine the flow for a given upstream head. Velocities profiles normal to the spillway chute slope along the centerline were taken at stations 0.0, 0.61, 1.2, 1.8,

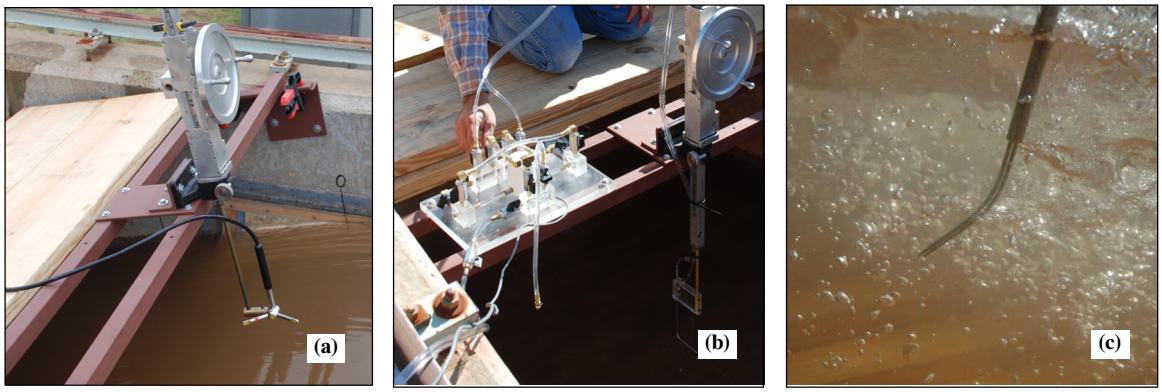

Figure 5. (a) ADV flow tracker, (b) Pitot tube with differential pressure transducer, and (c) two-tipped fiber optic probe.

2.4, 3.0, 3.7, 4.3, 4.9, and 5.5 m (0, 2, 4, 6, 8, 10, 12, 14, 16, and 18 ft) with the ADV when the velocities were within its recommended limits, with the PT for all stations on the chute, and with the FO probe when air entrainment was present. Two velocity profiles were taken with the PT and the FO probe along the stilling basin floor; these measurements were taken normal to the floor at stations 6.6 and 8.1 m (22 and 27 ft), respectively.

Results and Discussion

Chanson (1994b, 2002) performed numerous research studies on steep (i.e., 2(H):1(V) or steeper) stepped spillways. As a result, Chanson (1994b, 2002) developed a relationship that determines the inception point. A few points on flatter (i.e., 2(H):1(V) or flatter) stepped spillways were used in the development of this equation, yet Chanson (2002) still cautions the use of this equation on relatively flat slopes. Equation 1 is the inception point relationship developed by Chanson:

$$L_{i*} = 9.719(\sin\theta)^{0.0796}(F_*)^{0.713}h(\cos\theta) \quad (1)$$

where

L_{i*} = distance from the start of growth of boundary layer to the inception point of air entrainment
θ = channel slope
F_* = Froude number defined in terms of the roughness height ($F_* = q/[g(\sin\theta)\{h(\cos\theta)\}^3]^{0.5}$)
h = step height
q = unit discharge
g = gravitational constant.

Figure 1 illustrates L_i in relation to a spillway chute having a broad-crested weir. The origin point for length to the inception point is identified as the downstream edge of the broad-crested weir (fig. 1). This is also defined as the start of the growth of the boundary layer. A small amount of boundary layer development may occur upstream of this point on the smooth crest surface, but it is considered insignificant compared to the development that occurs downstream of this point on the stepped chute surface.

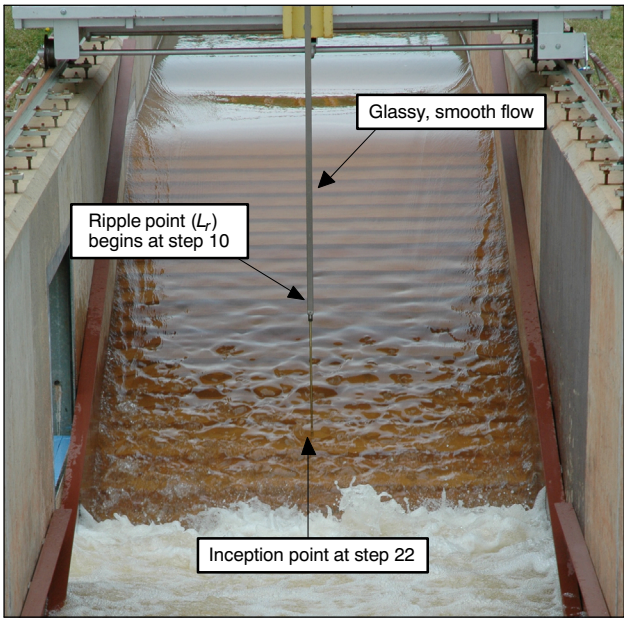

Figure 6. Flow observations detected under 0.28 m^3 s^{-1} m^{-1} (3.0 cfs ft^{-1}) flow conditions.

According to Hunt and Kadavy (2007, 2009), equation 1 can be used on slopes as small as 4(H):1(V) (θ = 14°) when the Froude surface roughness (F_*) ranges between 10 and 100. Hunt and Kadavy (2007) indicated that the location (i.e., station) of the air entrainment inception point can be detected by noting a visual change in the free surface. Figure 6 illustrates changes in the flow appearance during the tests. At locations slightly downstream of the spillway chute crest, the flow appears smooth and glassy. At step 10 (L_r = 1.6 m), a flow disturbance is noted in the form of a ripple, likely indicating that the turbulent boundary layer was nearing the free surface. This flow was considered transitional. When the flow became more irregular and erratic in behavior and the flow appeared frothy, the turbulent boundary layer was indicated to have reached the free surface. In the specific case of figure 6, this occurrence was recorded as the inception point, L_i, located at step 22 with an approximate L_i of 3.5 m (11.5 ft). Table 2 summarizes the average location of the inception point observed during the series of tests described herein as it compares to the inception point location for a range of discharges as calculated by equation 1. Table 2 also lists the Froude surface roughness (F_*) and the ripple point (L_r) location, which is the observed distance from the beginning of the turbulent boundary layer to the point where the turbulent boundary layer causes a slight disturbance (i.e., ripple) in the water surface. As table 2 illustrates, the observed inception point moves downstream with increasing discharge. These data show good agreement between the predicted and observed inception point locations for stepped spillway chutes as flat as 4(H):1(V). Differences between the observed and predicted inception points are likely due to the subjectivity of the visual observation. In particular, the observed and predicted inception points for the unit discharge of 0.62 m^3 s^{-1} m^{-1} (6.7 cfs ft^{-1}) showed a 14% difference. The inception point for this discharge was near the break in slope from the spillway chute to the stilling basin, so this slope change may have influenced the observed inception point location. The predicted inception point location for unit discharge of 0.11 m^3 s^{-1} m^{-1} (1.2 cfs ft^{-1}) is 21% larger than the observed inception point location, and this difference may be partially attributed to F_* equaling 10, the recommended minimum for the use of equation 1.

One of the advantages of stepped spillways is the energy dissipated in the spillway chute. As flow descends a stepped spillway chute, a roller develops on the steps. The momentum of the flow is transferred as the roller rotates the flow back into the main flow. As a result, significant energy is dissipated (Rice and Kadavy, 1996). To determine the energy loss in a spillway chute, the velocity must be known. Figure 7 presents typical velocity profiles measured with the ADV and PT at different stations within the spillway chute upstream of the inception point for a unit discharge of 0.28 m^3 s^{-1} m^{-1} (3.0 cfs ft^{-1}). The ADV and PT data are in excellent agreement with one another, giving confidence in the reliability of the equipment. Figure 7 also indicates that a pattern is present in the data. Based on Boes and Hager (1998) and Chanson (2000), the velocity profiles trend toward a one-sixth power law distribution near the inception point. Figure 8 illustrates this power law distribution as it is plotted with several of the velocity profiles for a unit discharge of 0.28 m^3 s^{-1} m^{-1} (3.0 cfs ft^{-1}). A one-sixth power

Table 2. Calculated and observed inception point data for each of the flows.

		Chanson (1994b)		Observed			
q (m^3 s^{-1} m^{-1})	F_*	L_{i*} (m)	Inception Point (step)	L_i (m)	Inception Point (step)	L_r (m)	Ripple Point (step)
0.82	75	7.0	basin	7.1	basin	4.1	26
0.62	57	5.7	36	6.6	basin	3.1	20
0.42	38	4.3	28	4.6	29	2.4	15
0.28	26	3.2	21	3.5	22	1.6	10
0.20	18	2.6	17	2.7	17	1.3	8
0.11	10	1.7	10	1.4	9	0.6	4

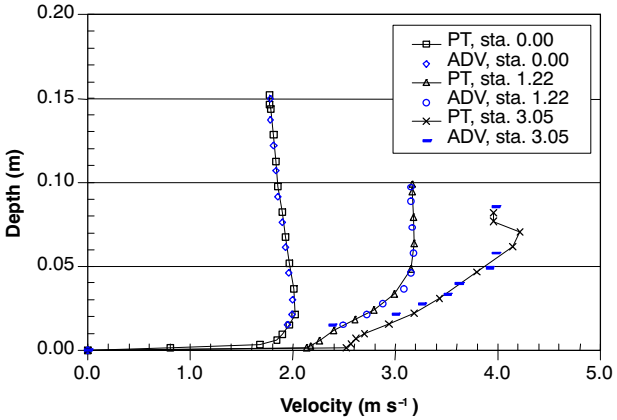

Figure 7. Velocity profiles using an ADV and PT for a unit discharge of 0.28 m^3 s^{-1} m^{-1} (3.0 cfs ft^{-1}).

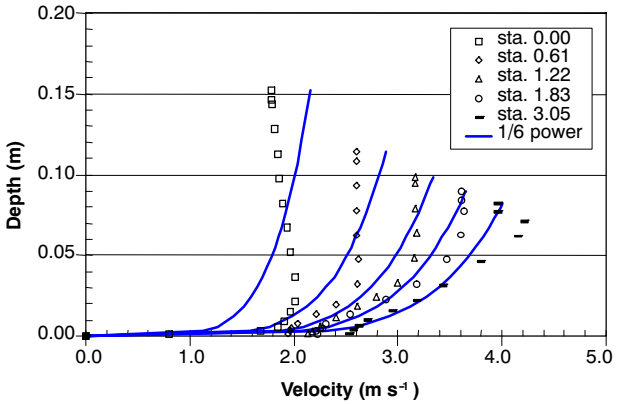

Figure 8. Velocity profiles for a unit discharge of 0.28 m^3 s^{-1} m^{-1} (3.0 cfs ft^{-1}) compared with a one-sixth power law distribution.

law distribution agrees more closely with the velocity profile as it approaches the inception point, located at L_i = 3.5 m (11 ft) for this flow.

The average velocity obtained from the velocity profiles was used to determine the relative energy loss on the spillway chute upstream of the inception point. The total energy loss to a given step relative to the step of interest is:

$$\Delta H = H_o - H \tag{2}$$

where

$$H_o = y_o + \frac{V_o^2}{2g}$$

$$H = y\cos\theta + \alpha\frac{V^2}{2g}$$

V = mean velocity
V_o = approach velocity
y_o = approach depth above datum
y = flow depth
θ = chute slope
g = gravitational acceleration
α = energy coefficient.

Figure 9 illustrates the energy loss parameters as they relate to the stepped spillway. The datum line is at the elevation of the step of interest. In many open-channel applications where the channel is of regular cross-section with fairly straight alignment, the energy coefficient (α) is assumed to equal unity because the effect of non-uniform velocity distribution on the computed velocity head and momentum is small (Chow, 1959). To determine the effect that the non-uniform velocity distribution has on the computed velocity head and momentum, equation 3 was used to determine the energy coefficient:

$$\alpha = \frac{\int v^3 dA}{V^3 A} \approx \frac{\sum v^3 \Delta A}{V^3 A} \tag{3}$$

where v is the velocity for an incremental area (ΔA) in the velocity profile, V is the mean velocity, and A is the area. Assuming two-dimensional flow that is uniform across the width, the area (A) can be replaced by the flow depth (y). Table 3 summarizes the energy data for the unit discharges 0.62, 0.28, and 0.11 m^3 s^{-1} m^{-1} (6.7, 3.0, 1.2 cfs ft^{-1}) and stations from the downstream crest edge to the stations near the inception point. As shown in figure 10, the energy coefficient ranges from 1.01 to 1.13. Figure 10 also illustrates the energy coefficient as it relates to a normalized length down the spillway chute (i.e., length from the downstream crest edge to the location of interest parallel to the spillway chute, L, normalized by the inception point location, L_i). The energy coefficient data presented in figure 10 show an approximate value of 1.08 at the inception point on average. The data scatter at the inception point is most likely associated with difficulty in measuring the flow depth with the ADV or measuring flow depths for low flows in general. An energy coefficient of 1.08 is still reasonable when compared to the values of 1.05 to 1.1 reported by Boes (1999) for fully air-entrained flows.

Figures 11 and 12 present the energy loss data in a similar manner as the energy coefficient data in figure 10. Figure 11 illustrates the relative energy loss versus the normalized length down the spillway chute observed during the test (L/L_i). Figure 12 shows the relationship of the relative energy loss versus the normalized length down the spillway chute using the inception point as calculated by equation 1 (L/L_{i*}). These figures demonstrate the linear relationship between

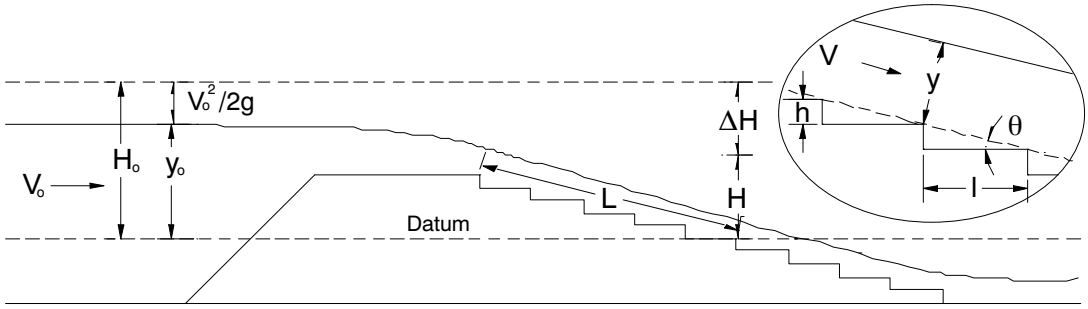

Figure 9. Energy loss parameters as they relate to the stepped spillway.

Table 3. Energy loss data and normalized length in the spillway chute for unit discharges of 0.62, 0.28, and 0.11 $m^3 s^{-1} m^{-1}$ (6.7, 3.0, 1.2 cfs ft^{-1}) based on PT data.

q ($m^3 s^{-1} m^{-1}$)	Station (m)	L (m)	H_o (m)	H (m)	$\Delta H/H_o$	L/L_i	L/L_{i*}
0.62	0.61	0.616	0.671	0.650	0.03	0.093	0.108
0.62	1.22	1.244	0.823	0.775	0.06	0.189	0.219
0.62	1.83	1.873	0.975	0.893	0.08	0.284	0.330
0.62	2.44	2.501	1.128	0.994	0.12	0.380	0.440
0.62	3.05	3.123	1.279	1.087	0.15	0.474	0.550
0.62	3.66	3.758	1.433	1.157	0.19	0.570	0.662
0.62	4.27	4.386	1.585	1.251	0.21	0.666	0.772
0.62	4.88	5.014	1.737	1.287	0.26	0.761	0.883
0.62	5.49	5.618	1.884	1.362	0.28	0.853	0.989
0.28	0.61	0.616	0.457	0.438	0.04	0.179	0.190
0.28	1.22	1.244	0.610	0.555	0.09	0.362	0.383
0.28	1.83	1.873	0.762	0.641	0.16	0.545	0.577
0.28	2.44	2.501	0.914	0.711	0.22	0.728	0.770
0.28	3.05	3.123	1.065	0.762	0.28	0.909	0.962
0.11	0.61	0.616	0.313	0.282	0.10	0.438	0.387
0.11	1.22	1.244	0.466	0.350	0.25	0.884	0.783

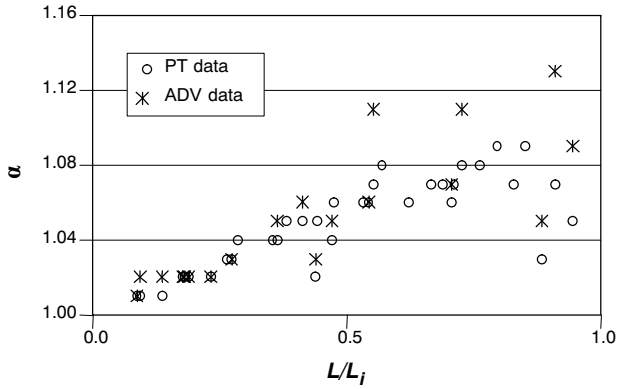

Figure 10. Energy coefficient (α) versus the normalized length (L/L_i) down the spillway chute.

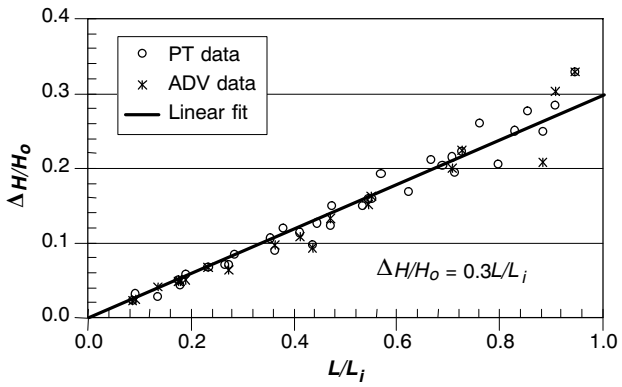

Figure 11. Relative energy loss versus the observed normalized length (L/L_i) down the spillway chute.

the relative energy losses versus the normalized length down the spillway chute. As L/L_i approaches the inception point (i.e., 1), the energy loss is approximately 0.30. When L/L_{i*} approaches 1, the energy loss is approximately 0.29. The closeness of these values demonstrates that equation 1 is appropriate for predicting the inception point for the experimental conditions (i.e., chute slope of 4(H):1(V) and F_* ranging between 10 and 100) described herein. Based on these findings, the relative energy loss at any point upstream of the inception point may be approximated by the following relationship:

$$\frac{\Delta H}{H_o} = 0.3\frac{L}{L_{i*}} \tag{4}$$

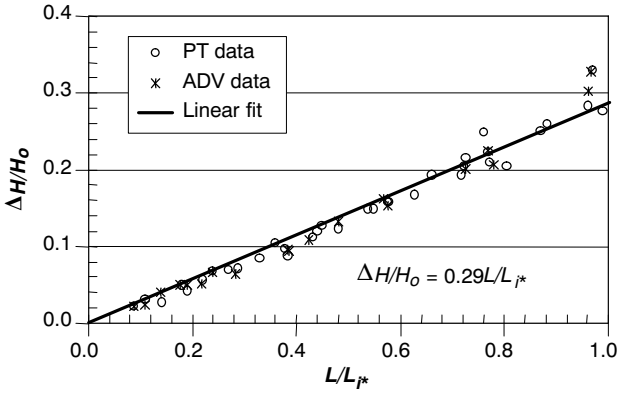

Figure 12. Relative energy loss versus the predicted normalized length (L/L_{i*}) down the spillway chute.

CONCLUSIONS

Stepped spillways provide substantial energy dissipation. When stepped spillways are applied to existing small earthen embankments, often the spillway chute is relatively short and the unit discharge is large. As a result, the inception point often occurs slightly upstream of the design tailwater or below the tailwater surface. Design engineers need information on the velocity entering the stilling basin and the energy dissipation that occurs in the spillway chute upstream of the inception point for stilling basin design. In this model study, the velocity profiles transition from uniform at the crest and approached a one-sixth power law distribution at the inception point for all tested flows. The inception point relationship developed by Chanson (1994a) can be used to determine the inception point location within the 4(H):1(V) stepped spillway chute when F_* ranges between 10 and 100 (Hunt and Kadavy 2009). The inception point location is important because it provides the design engineer with information on whether to take air entrainment into account in the design of the training walls. Additionally, the energy loss at any point upstream of the inception point may be determined and may be useful in the design of the stilling basin. Energy losses increase in a linear fashion from near zero at the crest to approximately 0.30 near the inception point for all tested flows. This research will assist engineers with the design of relatively short stepped spillway chutes as flat as 4(H):1(V) applied to embankment dams.

REFERENCES

Boes, R. M. 1999. Physical model study on two-phase cascade flow. In *Proc. 28th IAHR Congress*, Session S1. International Association for Hydro-Environment Engineering and Research.

Boes, R. M. 2000. Scale effects in modelling two-phase stepped spillway flow. In *Proc. Intl. Workshop on Hydraulics of Stepped Spillways*, 53-60. H. E. Minor and W. H. Hager, eds. Steenwijk, The Netherlands: A. A. Balkema.

Boes, R. M., and W. H. Hager. 1998. Fiber-optical experimentation in two-phase cascade flow. In *Proc. Intl. RCC Dams Seminar*. K. Hanson, ed. Denver, Colo.: Schnabel Engineering.

Boes, R. M., and W. H. Hager. 2003a. Two-phase flow characteristics of stepped spillways. *J. Hydraul. Eng. ASCE* 129(9): 661-670.

Boes, R. M., and W. H. Hager. 2003b. Hydraulic design of stepped spillways. *J. Hydraul. Eng. ASCE* 129(9): 671-679.

Chanson, H. 1994a. Hydraulics of skimming flows over stepped channels and spillways. *IAHR J. Hydraul. Res.* 32(3): 445-460.

Chanson, H. 1994b. *Hydraulic Design of Stepped Cascades, Channels, Weirs, and Spillways*. Oxford, U.K.: Pergamon.

Chanson, H. 2000. Characteristics of skimming flow over stepped spillways: Discussion. *J. Hydraul. Eng. ASCE* 125(4): 862-865.

Chanson, H. 2002. *The Hydraulics of Stepped Chutes and Spillways*. Steenwijk, The Netherlands: A. A. Balkema.

Chanson, H., and L. Toombes. 2002. Energy dissipation and air entrainment in a stepped storm waterway: An experimental study. *J. Irrig. and Drainage Eng. ASCE* 128(5): 305-315.

Chow, V. T. 1959. *Open-Channel Hydraulics.* Boston, Mass.: McGraw-Hill.

Christodoulou, G. C. 1993. Energy dissipation on stepped spillways. *J. Hydraul. Eng. ASCE* 119(5): 644-655.

Felder, S., and H. Chanson. 2008. Turbulence and turbulent length and time scales in skimming flows on a stepped spillway: Dynamic similarity, physical modeling, and scale effects. Queensland, Australia: University of Queensland, Division of Civil Engineering.

Gonzalez, C. A. 2005. An experimental study of free-surface aeration on embankment stepped chutes. PhD diss. Queensland, Australia: University of Queensland, Department of Civil Engineering.

Hunt, S. L., and K. C. Kadavy. 2007. Renwick dam RCC stepped spillway research. In *Proc. ASDSO Annual Meeting*, CD-ROM. Lexington, Ky.: Association of State Dam Safety Officials.

Hunt, S. L., and K. C. Kadavy. 2008. Velocities and energy dissipation on a flat-sloped stepped spillway. ASABE Paper No. 084151. St. Joseph, Mich.: ASABE.

Hunt, S. L., and K. C. Kadavy. 2009. Inception point relationship for flat-sloped stepped spillways. ASABE Paper No. 096571. St. Joseph, Mich.: ASABE.

Hunt, S. L., and K. C. Kadavy. 2010. Energy dissipation on flat-sloped stepped spillways: Part 2. Downstream of the inception point. *Trans. ASABE* 53(1): 111–118.

Hunt, S. L., K. C. Kadavy, S. R. Abt, and D. M. Temple. 2006. Converging RCC stepped spillways. In *Proc. 2006 World Environ. and Water Resources Congress, ASCE Conf.*, CD-ROM. Reston, Va.: ASCE.

Matos, J., K. H. Frizell, S. André, and K. W. Frizell. 2002. On performance of velocity measurement techniques in air-water flows. In *Proc. Hydraulic Measurements and Experimental Methods 2002*, CD-ROM. T. L. Wahl, C. A. Pugh, K. A. Oberg, and T. B. Vermeyen, eds. Reston, Va.: ASCE.

Peyras, L., P. Royet, and G. Degoutte. 1992. Flow and energy dissipation over stepped gabion weirs. *J. Hydraul. Eng. ASCE* 118(5): 707-717.

Rice, C. E., and K. C. Kadavy. 1996. Model study of a roller compacted concrete stepped spillway. *J. Hydraul. Eng. ASCE* 122(6): 92-297.

Takahashi, M., Y. Yasuda, and I. Ohtsu. 2005. Effect of Reynolds number on characteristics of skimming flows in stepped channels. In *Proc. 31st Biennial IAHR Congress*, 2880-2889. B. H. Jun, S. I. Lee, I. W. Seo, and G. W. Choi, eds. International Association for Hydro-Environment Engineering and Research.

Takahashi, M., C. A. Gonzalez, and H. Chanson. 2006. Self-aeration and turbulence in a stepped channel: Influence of cavity surface roughness. *Intl. J. Multiphase Flow* 32(12): 1370-1385.

Yasuda, Y., and I. Ohtsu. 1999. Flow resistance of skimming flow in stepped channels. In *Proc. 28th IAHR Congress*, Session B14. International Association for Hydro-Environment Engineering and Research.